Transactions of the Materials Research Society of Japan. Vol. 20

Impurity Concentration Measurement on MOSFET Cross-Section by Scanning Tunneling Spectroscopy-Atomic Force Microscopy

Kenji Yamazaki

LSI Laboratories, Nippon Telegraph and Telephone Corporation,
3-1 Morinosato-Wakamiya, Atsugi, Kanagawa 243-01, Japan

This paper reports a new method to evaluate the impurity diffusion layers in a metal-oxide-semiconductor field-effect transistor (MOSFET) cross-section. The technique integrates potential generation due to the photovoltaic effect and scanning tunneling spectroscopy-atomic force microscopy (STS-AFM). This potential distribution in a MOSFET cross-section can be fitted to the distribution of the impurity concentration measured by secondary ion mass spectroscopy (SIMS). The method is found to enable the observation of two-dimensional distributions of impurity concentration.

1 INTRODUCTION

In fabricating MOS devices, it is important to evaluate the impurity-diffusion-layer and channel structures, because these structures significantly affect device electronic characteristics and reliability. One-dimensional evaluations of these structures are very often performed by SIMS and spreading resistance measurement. Two- (or three-) dimensional evaluations are, however, essential[1] to link the device fabrication conditions to process/device simulations, and have been performed by using electron beam induced current (EBIC)[2] and etching delineation methods[3] with various kinds of acid solution. However, these two-dimensional methods lack the resolution for evaluating the advanced devices currently being developed or that will emerge in the near future.[1]

In attempts to satisfy these requirements, many groups have proposed improved techniques involving, for example, transmission electron microscopy[4]/scanning probe microscopy[5,6] after dopant-sensitive etching, scanning capacitance microscopy (SCM),[7] and Kelvin probe force microscopy (KFM).[8] The resolutions of these methods, however, don't seem to be sufficient yet for the requirement. Moreover, the reproducibility of the used etching methods is inadequate, and the techniques using SCM and KFM, while having recently been improved remarkably, are still under development.[7,8].

Consequently, we have applied our STS-AFM technique[9], which can directly observe electronic properties and topography with high resolution, to the evaluation of impurity concentration distribution in order to get good reproducibility and precision. We obtain a MOSFET cross-section image of the potential distribution caused by the photovoltaic effect. This image is converted to the two-dimensional distribution of impurity concentration.

2 EXPERIMENT

The apparatus controls the vertical relative position between the tip and specimen by contact AFM, and measures a current-voltage (I-V) curve at each (X,Y) point. The topographic image and electronic-property images derived from the I-V characteristics can therefore be obtained simultaneously.[9]

During measurement, part of the laser beam used for detecting the distortion of the AFM cantilever is aimed around the measured region of the MOSFET cross-section as shown in Fig. 1. This is done to produce a potential distribution across the well layer and diffusion layers caused by the photovoltaic effect, as in a solar cell. Although I-V curves are in fact measured, a potential image is obtained by mapping the value of the bias voltage with no current.[10] In this sense, this method is a kind of scanning tunneling potentiometry.

The potential difference due to the photovoltaic effect is often written as simple theoretical expressions. For the degenerated n-type region on p-type silicon, the potential difference with no current can be written as $\Delta\Phi \sim kT \ln \frac{N_A N_{ex}}{n_i^2}$, as in a p-n junction solar sell, where N_A is the acceptor impurity density in the well, N_{ex} is the excited carrier density, n_i is the intrinsic density, k is Boltzmann's constant, and T is the tempera-

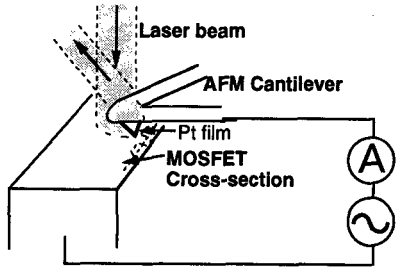

Figure 1. Experimental set up. The laser beam produces potential due to the photovoltaic effect.

ture. Figure 2 shows good agreement between the theory and the experimental results measured by the STS-AFM.

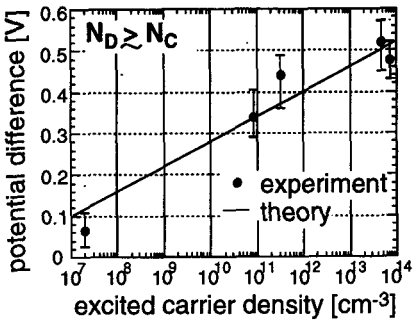

Figure 2. The relationship between the potential difference and the excited carrier density. The experimental results are in good agreement with the photovoltaic effect theory.

An LSI chip with n-MOS transistors was used for the experiment. The chip was cut and bonded, and its cross-section was mirror-polished in order to make it flat. We could not detect enough current for this cross-section because of contamination due to the polishing. To remove the contamination, it has to be cleaned by Argon-ion sputtering. The sputtering, however, changes the electronic properties of the specimen probably because a lot of surface states as well as crystal damage are generated. For an n-type over p-type silicon surface, the potential difference due to the photovoltaic effect and the current ratio at −1-volt bias voltage change from high values to low ones because of the sputtering (Fig. 3). These changes are consistent with the increasing number of surface states, and would make a high-resolution evaluation quite difficult. However, by chemical etching with NH_4OH:H_2O_2:H_2O = (1:1:6), the damaged layer can be removed, and the electronic properties recover as shown in Fig. 3. Finally, the specimen was dipped in HF solution to remove native oxide caused by the etching solution. Before the measurement, the specimen was exposed to air to ensure a native oxide film formed on the silicon surface.[9,10]

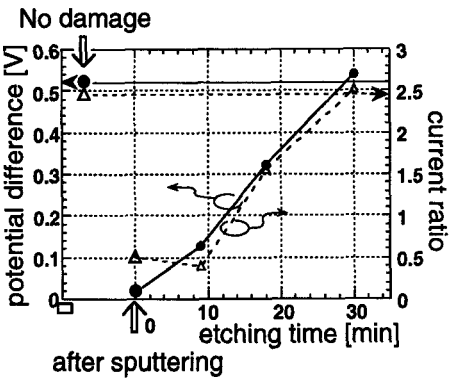

Figure 3. Electronic damage caused by Ar^+ sputtering is removed by the chemical etching.

3 RESULT

Figures 4(a) and (b) are the STS-AFM topographic image and potential image of the n-MOS cross-section. The topographic image shows the shape of the gate electrode and the edge of the crystal silicon. The potential image shows the potential distribution continuously changes from the p-type well to the n-type diffusion layers. In the upper green part of this image, potential can not be defined because there is no current. By overlaying these images, the relative position between the gate and the diffusion layers can be seen.

Taking the potential distribution along the depth direction in Fig. 4(b) and the concentration profile measured by SIMS for a similar specimen, the former can be fitted to a logarithmic expression of the latter over the wide range below the degenerated concentration (Fig. 5). The correspondence is good and is consistent with the following theoretical understanding.

4 THEORY AND DISCUSSION

Since laser beam irradiation excites many electrons and holes in a semiconductor, band bending and the Fermi level become different from those of a non-irradiated specimen. In the excited region, the laser beam increases the minimum density of holes and electrons up to a value defined

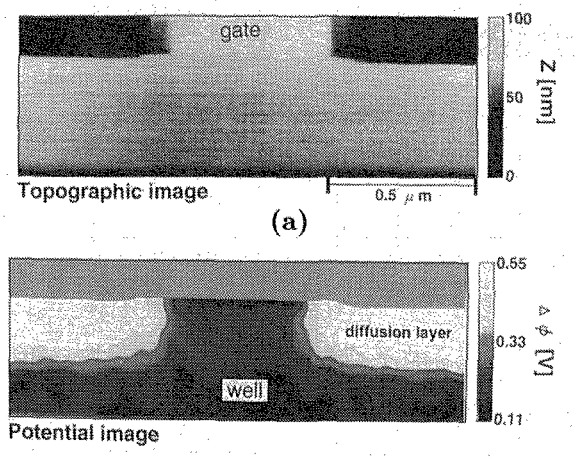

Figure 4. Topographic (a) and potential (b) images for n-MOS cross-section. By overlaying these images, one can see the relative position between the gate and the diffusion layers.

by the laser intensity. Then, the concentration distribution for holes and electrons changes and band bending becomes weak. Moreover, quasi-Fermi levels for electrons and holes separate from the Fermi level in thermal equilibrium.[10]

As shown in Fig. 2, for the degenerated n-type region on a p-type well (Region III), the potential difference depends not on the impurity concentration, as long as it's degenerated, but on the exited carrier density and the acceptor density. For the region where n-type impurity concentration is very small (Region I), the Fermi level of the tip should be close to the quasi-Fermi level for holes

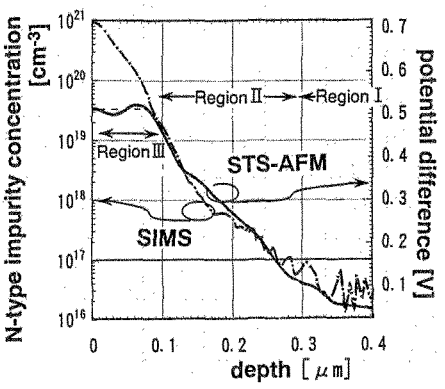

Figure 5. The potential distribution along depth direction corresponds to SIMS data.

under the condition of no current. The measured potential therefore becomes around zero.[10]

For the n-type medium concentration region on a p-type well (Region II), the potential measurement is explained using the band diagram shown in Fig. 6. Under the condition of no measured current, the ratio of the electrons and holes on the extreme surface of the specimen becomes constant. Then the bias voltage $\Delta\Phi$ can be written as $\Delta\Phi \sim c\frac{kT}{2e} \ln \frac{n}{p_{ex}} + C'$ with some approximations,[10] where n is the electron density and c and C' are constants. Therefore, the measured potential has a linear relationship to the logarithm of the electron density in this region.

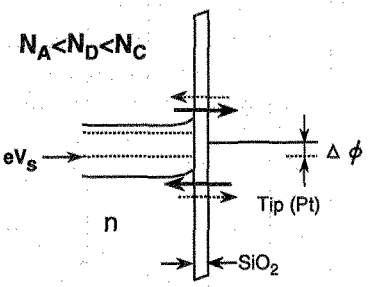

Figure 6. A band diagram for medium concentration. This shows how potential is measured when tunneling current balances.

Generally, electronic measurement methods for impurity concentration measure carrier density rather than impurities themselves. Although majority carrier density decreases a lot compared to the impurity density in depletion layers, the simulations for one-dimensional abrupt junctions (Fig. 7) show that the depletion layer widths are reduced, and that the majority carrier densities become closer to the impurity densities, depending on the excited carrier density. Therefore, the relation between the measured potential and the logarithm of the impurity concentration is linear in most of the important region for MOS device evaluation.

From the theoretical explanation above and the fitting between the potential and the concentration in Fig. 5, we can draw a conversion curve for this specimen (Fig. 8). From this conversion curve, the potential image (Fig. 4 (b)) can be replaced by a contour image (Fig. 9).

Further theoretical consideration shows that the dopant concentration sensitivity of our method depends on the acceptor density in the well and is better than 2×10^{17} cm^{-3} in this MOSFET, and that the spatial resolution of this method is better than 10 nm for high concentra-

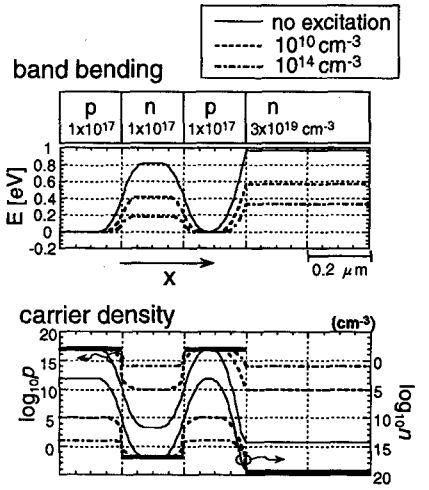

Figure 7. Simulations for one-dimensional abrupt junctions. Excited carriers reduce the depletion-layer width and make majority carrier density closer to the impurity density.

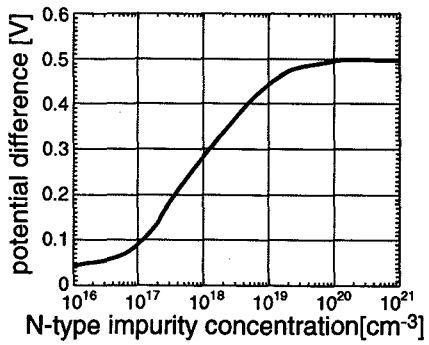

Figure 8. A conversion curve from the potential to the impurity concentration.

tions and better than several tens of nm for a concentration of 10^{17} cm^{-3}.[10]

5 CONCLUSION

We represent a new method to evaluate the impurity diffusion layers in a metal-oxide-semiconductor field-effect transistor (MOSFET) cross-section. The technique integrates potential generation due to the photovoltaic effect and scanning tunneling spectroscopy-atomic force microscopy. This potential distribution on a MOSFET cross-section can be fitted to the distribution of the impurity concentration measured by secondary ion mass spectroscopy (SIMS). The method enables the observation of two-dimensional distributions of impurity concentration. Our method represents an efficient way to clarify the correspondence between semiconductor fabrication conditions and process/device simulations.

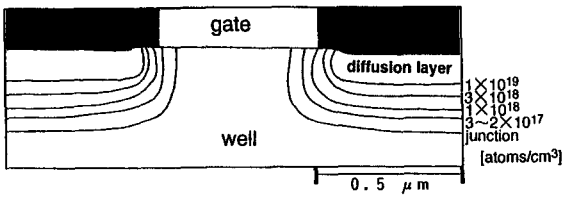

Figure 9. Impurity concentration image derived from the potential image (Fig. 4 (b)).

acknowledgment

I would like to thank Dr. Shigeru Nakajima for much useful advice and encouragement, and Mr. Yoshiyuki Sato for suggesting this work in the first place and providing important information like SIMS data. The author also wishes to acknowledge Dr. E. Arai, Dr. A. Iwata, Dr. S. Ishihara, and Dr. K. Izumi for their support and encouragement.

REFERENCES

1. A. C. Diebold and M. Kump, J. Vac. Sci. Technol., B **14** (1996) 196.
2. For example, H. K. Schink and H. Rehme, Electronics Letters, **19** (1983) 385.
3. For example, S. T. Ahn and W. A. Tiller, J. Electrochem. Soc., **135** (1988) 2370.
4. D. M. Maher and B. Zhang, J. Vac. Sci. Technol., **B 12**, (1994) 347.
5. T. Takigami and M. Tanimoto, Appl. Phys. Lett., **58**, (1991) 2288.
6. V. Raineri *et al.*, Appl. Phys. Lett., **64**, (1994) 354.
7. G. Neubauer *et al.*, J. Vac. Sci. Technol., B **14** (1996) 426.
8. M. Tanimoto and O. Vattel, J. Vac. Sci. Technol. B **14** (1996) 1547.
9. K. Yamazaki and S. Nakajima, Jpn. J. Appl. Phys. **33**, 3743 (1994).
10. K. Yamazaki, Special Issue of Bulletin of the Research Institute of Electronics, **30** No. 3, Shizuoka University, Hamamatsu, Japan, *in printing.*
11. R. J. Hammers and K. Markert, J. Vac. Sci. Technol. **A 8**, 3524 (1990).